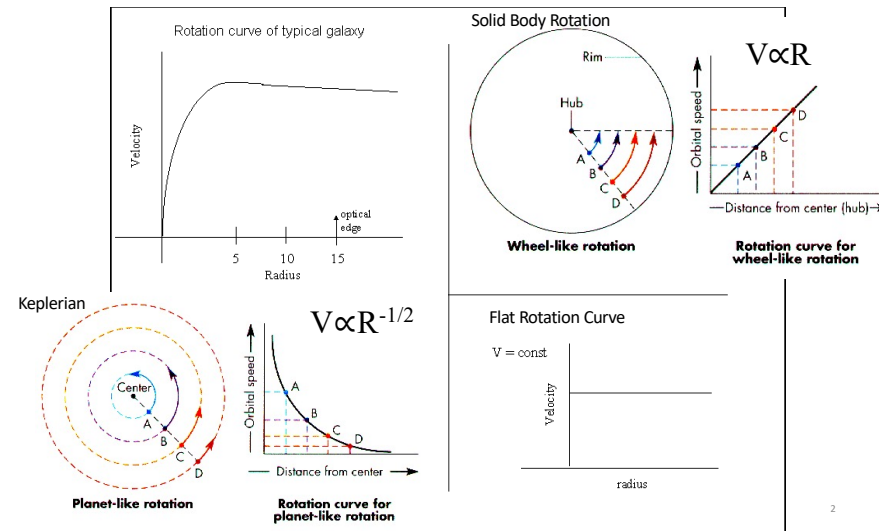


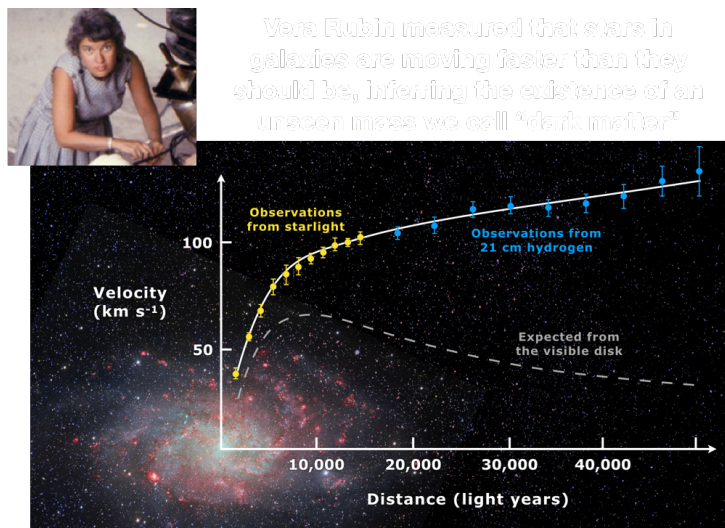
$$GMm/R^2 = mV^2/R$$

$$M(< R) \propto V^2 R$$

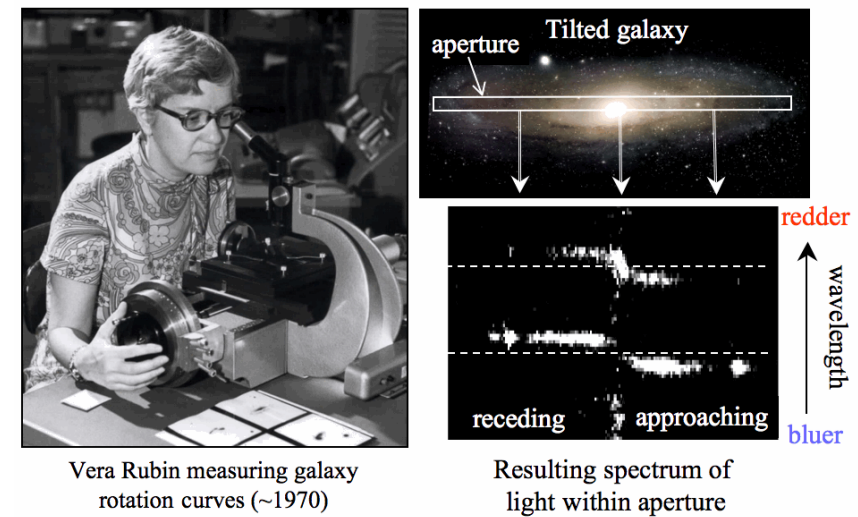
$$v_c(R) = \sqrt{GM(< R)/R}$$



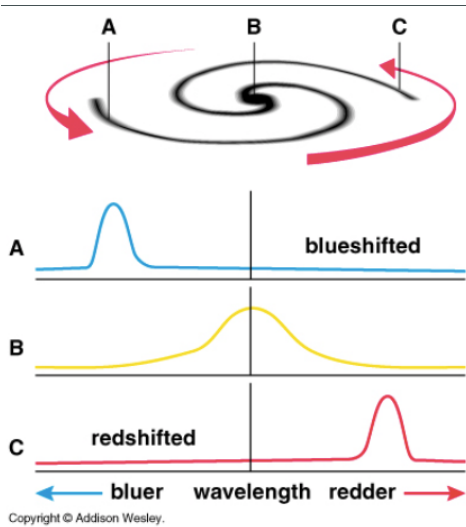
2



3

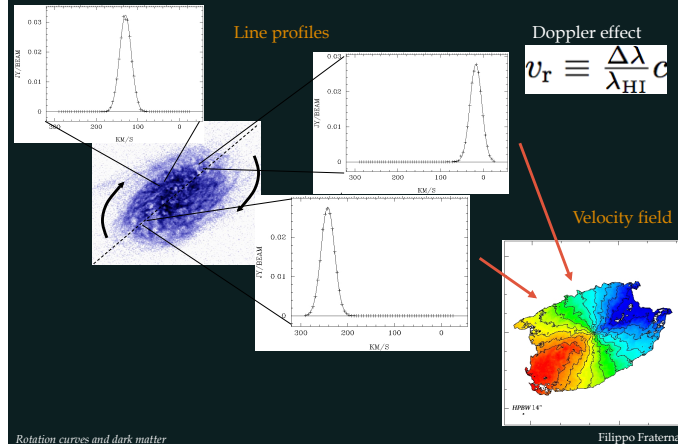


4



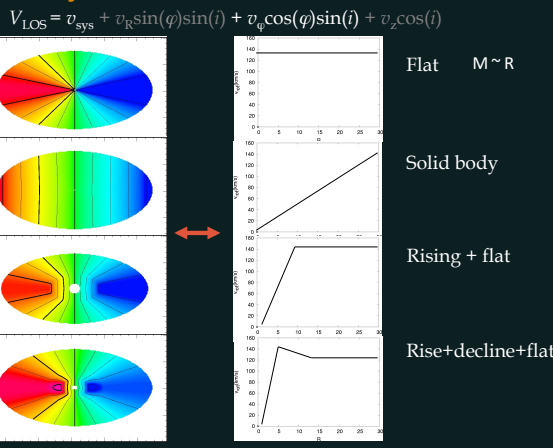
5

Rotation of a galactic disc



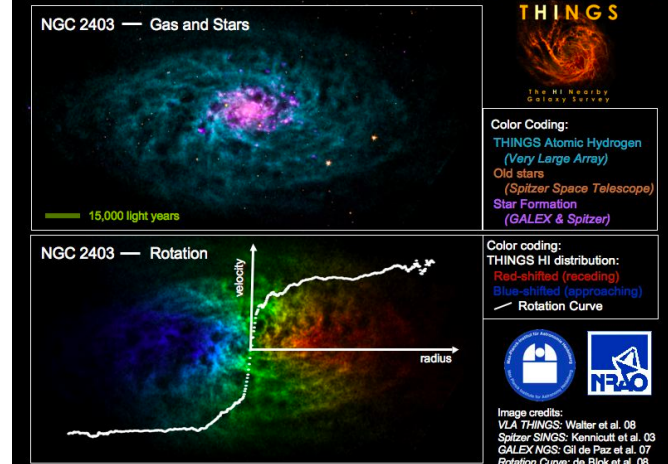
6

Velocity fields versus rotation curves



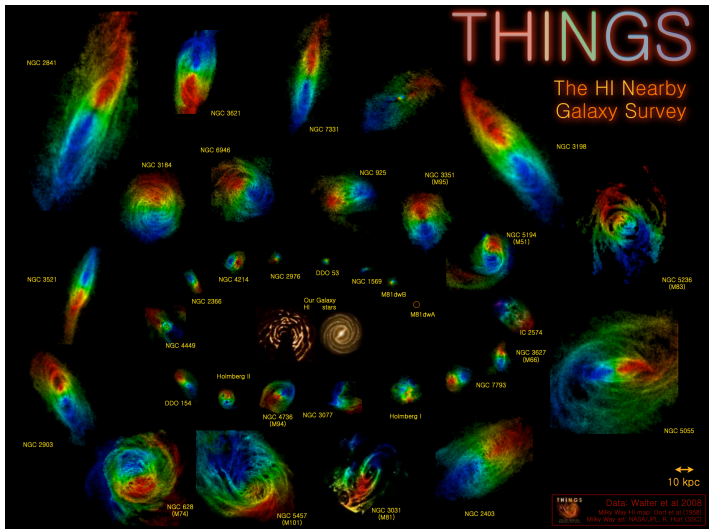
7

Galaxy Dynamics in THINGS — The HI Nearby Galaxy Survey



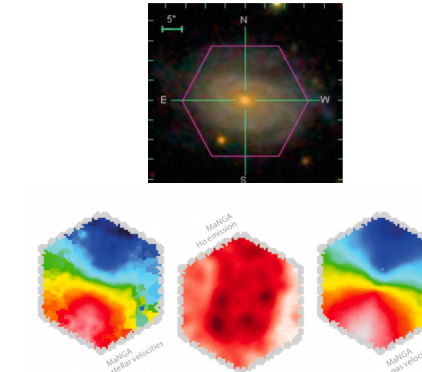
8

8



9

IFUs : SDSS IV & MANGA



Credit: Francesco Belfiore, Univ. of St Andrews Print & Design.

Bundy + 2015



MaNGA obtains spectra across the entire face of target galaxies using custom designed fiber bundles. The bottom right illustrates how the array of fibers spatially samples a particular galaxy. The top right compares spectra observed by two fibers at different locations in the galaxy, showing how the spectrum of the central regions differs dramatically from outer regions.
Image Credit: Dana Berry / SkyWorks Digital Inc., David Law, and the SDSS collaboration.

10

Cores vs. Cusps

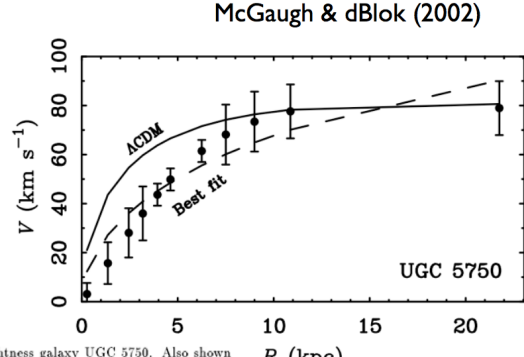


Fig. 1.— The rotation curve of the low surface brightness galaxy UGC 5750. Also shown are the best fitting NFW halo parameters ($c = 2.6$, $V_{200} = 123 \text{ km s}^{-1}$; dashed line) for the limiting case of a zero mass (minimum) disk, and what the NFW halo should look like for a galaxy of this rotation velocity in the standard Λ CDM cosmology ($c = 10$, $V_{200} = 67 \text{ km s}^{-1}$; solid line). The excess of the solid line over the data illustrates the cuspy halo problem. Though an NFW fit can be made (dashed line), it is a poor description of the data, and requires a very low concentration ($c = 2.6$ does not occur in any plausible cosmology). These problems become more severe as allowance is made for stars (BMR; BB).

11

Leiden/Dwingeloo & IAR HI Surveys: $b = 0$

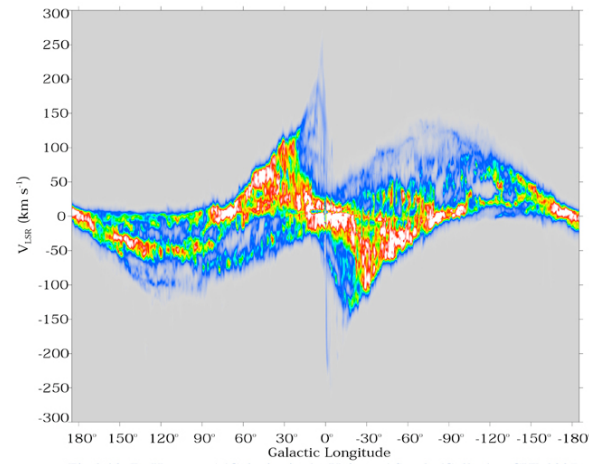


Fig. 2.20 (D. Hartmann) 'Galaxies in the Universe' Sparke/Gallagher CUP 2007

In the plane of the disk, the intensity of 21 cm emission from neutral hydrogen moving toward or away from us with velocity V_{LSR} measured relative to the local standard of rest.

12

Galactic rotation: a gas cloud at marked points. Gas cloud at d with longitude l and Galactocentric radius R , at distance d from the Sun, orbits with speed $V(R)$. The line of sight is closest to the Galactic center at the tangent point, C.

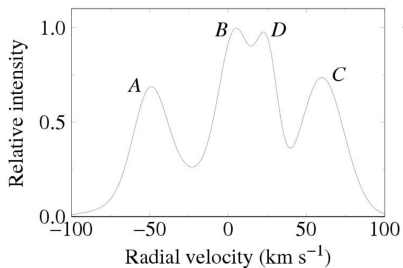


Figure 1: The tangent point method

13

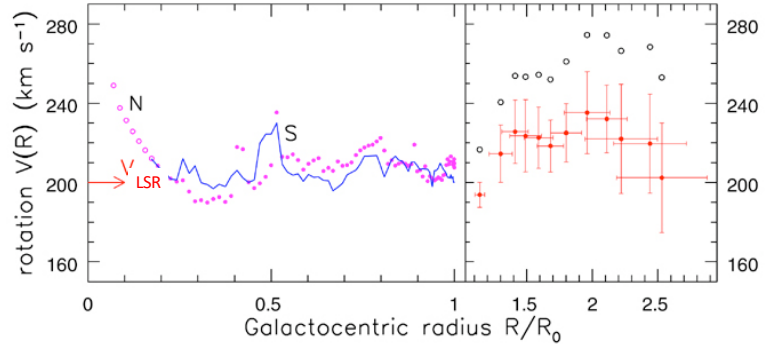
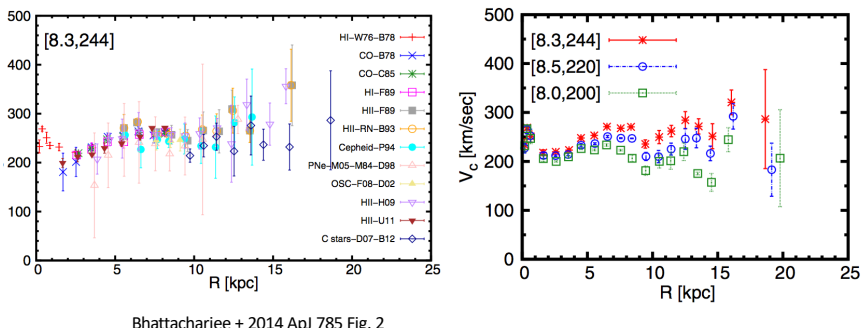


Fig 2.21 (Burton, Honma) 'Galaxies in the Universe' Sparke/Gallagher CUP 2007

Left: the Milky Way's rotation from the tangent-point method taking $V_{\text{LSR}} = 200 \text{ km/s}$; dots show velocities of northern HI gas with $l > 270^\circ$; the curve gives results from southern gas at $l < 90^\circ$. The tangent-point method fails at $R < 0.2 R_\odot$ (open circles) because the gas follows oval orbits in the Galactic bar. Right, the rotation speed of the outer Galaxy, calculated for $V_{\text{LSR}} = 200 \text{ km/s}$ (filled circles) and for $V_{\text{LSR}} = 220 \text{ km/s}$ (open circles); crosses show estimated errors.

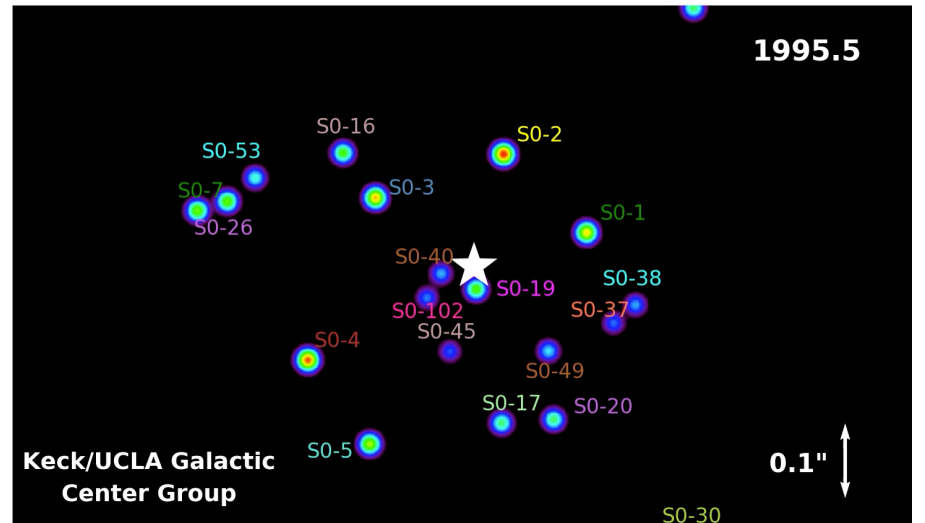
14



Bhattacharjee + 2014 ApJ 785 Fig. 2

Left: Rotation curves of the Galaxy obtained using the various different disk tracer samples (HI, Cepheids, HII regions, Carbon stars, CO) assuming Galactic constants $[(Ro/\text{kpc}), (\text{VLSR}/\text{km s}^{-1})] = [8.3, 244]$.

Right: averaged rotation curves obtained by weighted averaging over the combined V_c data from all the disk tracer samples in left panel, for three different sets of values $[(Ro/\text{kpc}), (\text{VLSR}/\text{km s}^{-1})]$ as indicated



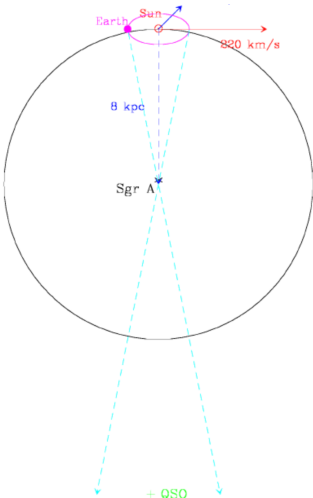
16

Proper Motion of Sgr A*

$$\mu_{SGRA*} = -6.379 \pm 0.026 \text{ mas/yr}$$

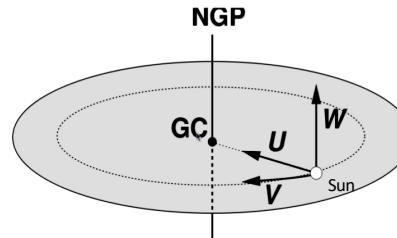
Reid & Brunthaler 2004, VLBI measurements of SgrB2

$$v_{tan} = 4.74 \frac{\mu}{\text{mas/yr kpc}} \frac{R_o}{\text{kpc}} = V_{LSR} + v_\odot$$



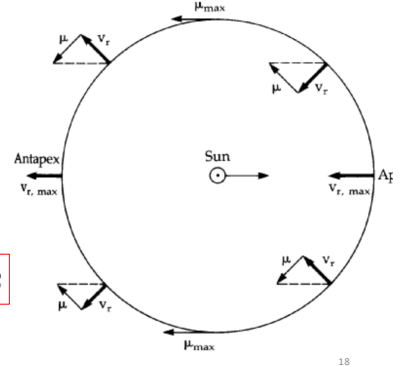
Peculiar motion of the Sun wrt LSR

See Carroll & Ostlie Chap 24



Solar Peculiar Motion: Schonrich 2010

$$(u, v, w)_\odot = 11.1 \pm 1.23, 12.24 \pm 2.05, 7.25 \pm 0.62$$

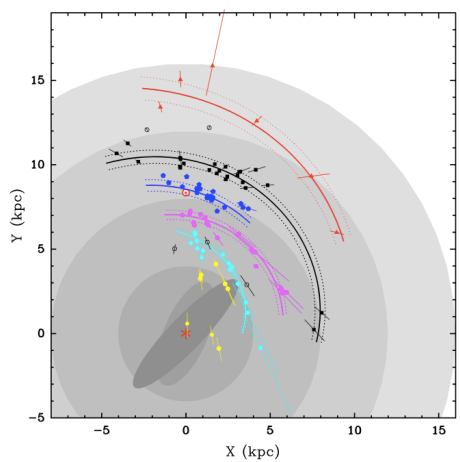


18

18

Galactic Center Distance: Parallax to Star Forming Regions

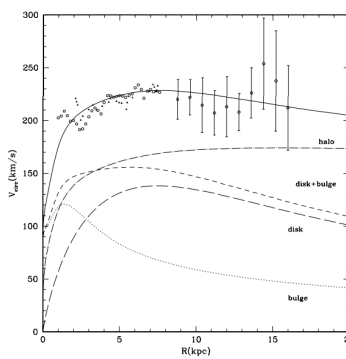
$\text{lo} = 8.34$
 $: 0.16 \text{ kpc}$
eid +2014 ApJ 783



Location of high-mass star forming regions (HMSFRs) with trigonometric parallaxes by VLBA. Galactic center (red asterisk) is at (0,0) and Sun (red sun symbol) is at (0,8.34).

HMSFRs were assigned to spiral arms based on association with structure seen in plots of CO and HI emission : Scutum Arm (cyan octagons); Sag Arm (magenta hexagons); Local arm (blue). Distance error bars are indicated. Galactic rotation is clockwise

22



Klypin+2002
Data needs to be Scaled to account for new R0

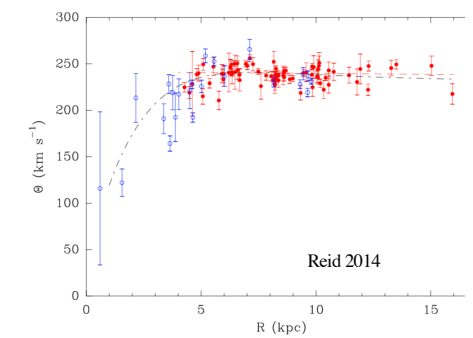
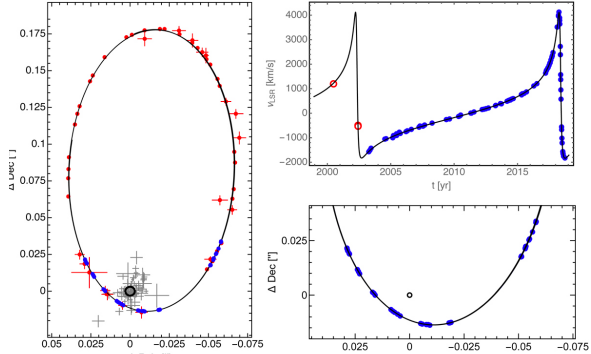


Figure 4. Rotation curve for all high mass star forming regions with measured parallax and proper motion in Table 1. Plotted is the circular velocity component, Θ , as a function of Galactocentric radius, R . The transformation from heliocentric to Galactocentric frames uses the parameter values of fit A5, but only on sources with $R > 4$ kpc; these sources are plotted with filled \circ symbols. The sources not used in the final fitting are plotted with open \circ symbols. The dashed red line indicates the fitted rotation curve (model A given by $\Theta = \Theta_0 - 0.2(R - R_0) \text{ km s}^{-1}$, where R and R_0 are in kpc. The dash-dot black line is the best fit “universal” rotation curve (model D1) spiral galaxies (Persic et al. 1996), which begins to capture the clear velocity down turn for stars with $R \lesssim 5$ kpc.

23

Galactic Center Distance: Fitting the orbit of S2

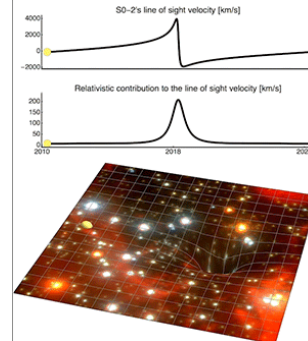


Abuter + 2019 GRAVITY Collaboration

$$R_o = 8.178 \pm 0.013_{\text{stat}} \pm 0.022_{\text{sys}}$$

Orbit of S2. *Left:* on-sky view of the astrometric data (red: AO data, blue: GRAVITY data) in the down-sampled version with the best-fit orbit (black ellipse). The black circle marks the position of Sgr A*. The locations of previous AO-based flares agree with that position (gray crosses). *Right top:* radial velocity data of S2 together with the best-fit orbit. The blue data are from the VLT, the red are earlier epochs from the Keck data set (Ghez et al. 2008). *Right bottom:* zoom into the on-sky orbit in 2017 and 2018, showing the GRAVITY data that have error bars smaller than the symbol size.

24

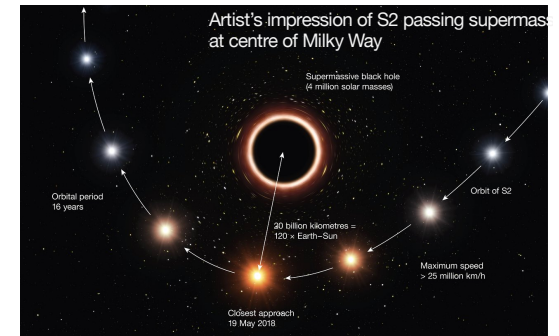


UCLA Team:
Do + 2019

GRAVITY Collab
Abuter+2018

As the star S2-2 nears our galaxy's supermassive black hole (orbit exaggerated), the light it emits has to climb out of the gravitational potential well, losing energy. This process reddens the light. The star's motion along our line of sight also shifts the light's wavelengths, and so astronomers measure both shifts in km/s.

Credit: Aurelien Hees / Keck UCLA Galactic Center Group



25

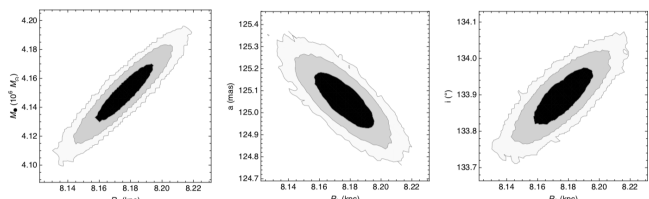


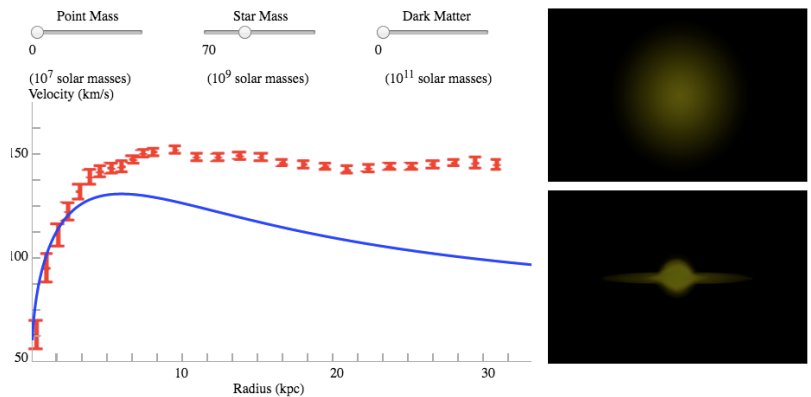
Fig. 2. Selected posterior densities as obtained from the MCMC sampler with $N = 200\,000$, here for the noise model data set. The contour lines mark the 1, 2, and 3σ levels. We only show the diagrams with the strongest correlations. All parameters are well determined (see Appendix D).

Abuter + 2019 GRAVITY Collaboration

26

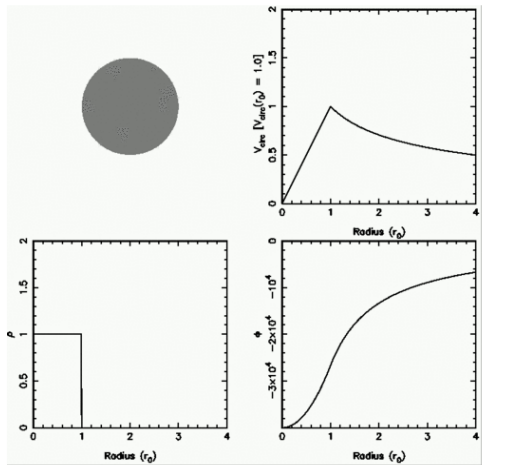
Try for yourself:

<http://wittman.physics.ucdavis.edu/Animations/RotationCurve/GalacticRotation.html>



28

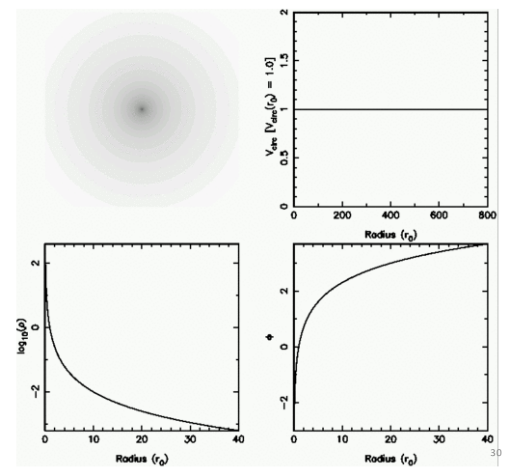
Uniform Sphere



$$\rho(r) = \frac{M}{4\pi r^3}$$

$$\Phi(r) = -GM/r$$

Isothermal Sphere

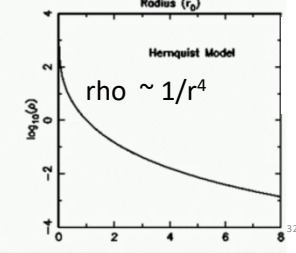
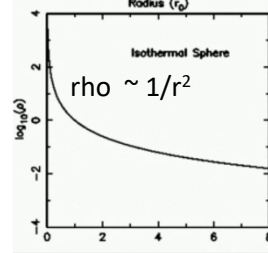
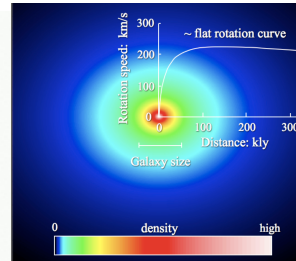
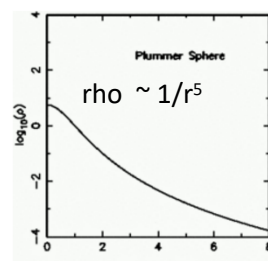
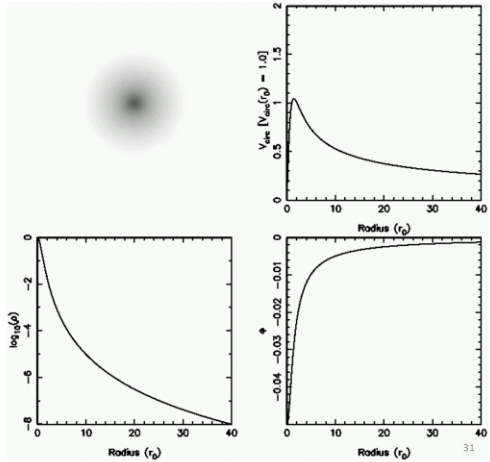


30

Plummer model

$$\rho(r) = \frac{M}{4/3\pi a^3} (1.0 + r^2/a^2)^{-5/2}$$

$$\Phi(r) = -GM/\sqrt{r^2 + a^2}$$



Hernquist 1990 Profile

$$\rho(r) = (M/2\pi) \frac{a}{(r(r+a)^3)}$$

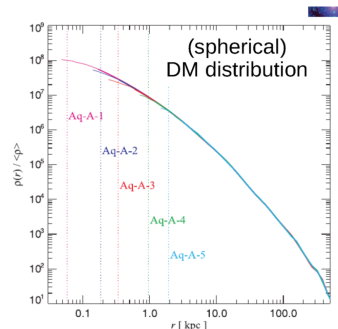
$$\Phi(r) = -GM/(r+a)$$

32

$$\rho \sim 1/r^3$$

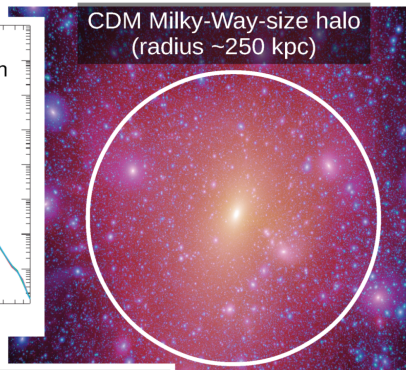
NFW

$$\rho(r) = \frac{\rho_0}{r/r_s(1+r/r_s)^2} \quad \Phi_{\text{NFW}}(r) = -\sigma_N^2 \frac{\ln(1+r/r_s)}{r/r_s} \quad \sigma_N = 4\pi G \rho_0 r_s^2$$



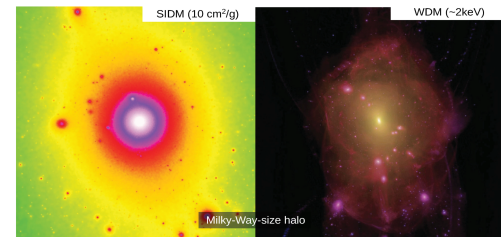
Zavala & Frenk 2019 Review

CDM Milky-Way-size halo
(radius ~250 kpc)

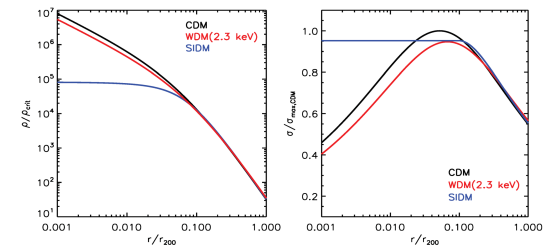


33

More complications



Zavala & Frenk 2019 Review



34

34